Since January 2020 Elsevier has created a COVID-19 resource centre with free information in English and Mandarin on the novel coronavirus COVID-19. The COVID-19 resource centre is hosted on Elsevier Connect, the company's public news and information website.

Journal of Infection 84 (2022) e133–e136

Contents lists available at ScienceDirect

Journal of Infection

journal homepage: www.elsevier.com/locate/jinf

Letter to the Editor

Targeting omicron and other reported SARS-CoV-2 lineages by potent inhibitors of main protease 3CL Mpro: Molecular simulation analysis

Dear editor,

Besides vaccines, anti-SARS-CoV-2 drugs are urgently needed to cease the pandemic. Clinical use of its protease inhibitor therapy for COVID-19 has been reported in this Journal by Deng et al.[1] The SARS-CoV-2 3CL Mpro protease plays essential roles in viral replication, transcription, inducing cytokines IL-1β, IL-6, TNF-α, in Calu-3 and THP1 cells.[2] To comment on the utilization of protease inhibitors, we here identify and probe other potential candidates besides Arbidol and LPV/r.[1] We picked the Mpro structure in full-length that retains a cysteine containing catalytic pocket, unlike chymotrypsin-like enzymes and performed structure-based virtual screening and molecular dynamic simulation on 25 FDA approved antiviral and 4000 unknown lead molecules. Among the reported inhibitors silymarin, ferulic acid and p-coumaric acid identified as best binders with overall energies of -15.0411 Kcal/mol, -10.6320 Kcal/mol and -10.7634 Kcal/mol, respectively. Contrary, from the list of the unknown compounds, ZINC64219754, ZINC64219742 and ZINC64219736 showed binding affinities of -11.6969 Kcal/mol, -11.1067 Kcal/mol and -10.7840 Kcal/mol (Table 1). In line, silymarin, ferulic acid and p-coumaric acid have already shown high potency as antiviral drugs against flaviviruses, togaviruses, adenoviruses and dengue virus.[3,4] Silymarin engaged Thr26, Asn142, Ser144, Cys145 and His163 and contributed to six hydrogen bonds and van der Waal (vdW) interactions. In the case of Ferulic Acid and p-coumaric acid, besides vdW interactions, six and four hydrogen bonds were observed, respectively. Interestingly, all the three known compounds stayed consistent in capturing the catalytic residue Cys145, which was recently a reported case with MG-132 against 3CL Mpro.[5]

The docked ZINC64219754 depicted two hydrogen bonds coupled with vdW interactions, where one of the interactions was achieved with catalytic His41 compared to the Cys145, observed in known drugs. The presence of multiple carboxylate groups makes the environment of the compound more electrophilic and facilitates the formation of electrostatic interactions with active site residues. The imidazole Nε1 atom of His41 forms a hydrogen contact with conserved H2Ocat molecule whereas the Nε2 atom engaged carbonyl oxygen of the inhibitor. To our interest, the compound ZINC64219742 captured both the catalytic residues, His41 and Cys145 at distances of 2.5 Å and 3.1 Å. Finally, the interaction pattern of ZINC64219736 was observed to constitute three hydrogen bonds and vdW interaction with amino acids residues of His41, Asn142, Gly143 and His164 at the range of 2.1 – 2.9 Å (Fig. 1A). Overall, our docking analyses suggest that all the three unknown binders retain the capability to arrest the catalytic residues and in particular ZINC64219742 indicated the ability of capturing the dyad.

Accessing the stability of protein–ligand interactions and ligand-induced changes in the protein structure, all the six 3CL Mpro docked complexes were tested in 50ns each of MD simulation. All the complexes successfully attained the equilibration state and stayed in the RMSD range of 1 – 4 Å, suggesting a stable behavior of the Mpro with all the six compounds (Fig. 1B). Analyzing the interaction panel for ferulic acid, we found that only two H-bond interactions with Glu166 and Gly143 stayed stable in simulation, while interaction with Cys145 and Ser144 were lost in the first 2ns range. Contrary, two new and relatively stable interactions were attained with Phe140 and His163. On the other hand, Silymarin showed the best fitness and achieved few more H-bond interactions but interestingly all the interactions remained highly stable. Apart from Glu166, p-coumaric acid replaced all the interactions achieved in docking with Gln189, His41, Ser46 and Tyr54. The ZINC compounds, ZINC64219736 formed two new stable contacts with Asn277 and Asn238 along with other part time interactions but unfortunately have lost all the contacts observed in docked complexes. Similar to its docked complex, ZINC64219742 and ZINC64219754 stayed in the active pocket region through hydrophobic interactions (Fig. 2A).

To conclude, status of the tested compounds during simulation, silymarin appeared the most native compound in the active pocket of Mpro forming H-interactions, followed by the p-coumaric and ferulic acid. Contrary, all the three compounds from the ZINC database stayed in the active-pocket relying on hydrophobic interactions. It is noteworthy that all the complexes in simulation have attained equilibrated state whereas the RMSF profile did not indicate any spontaneous jump, suggesting the stable nature of these compounds in the active pocket region.

Many variants of SARS-Cov-2 have been reported since pandemic including alpha to omicron. Based on the observed number of mutations in these variants, we found that only beta and omicron variants harbor single mutations each, i.e., K90R and P132H, respectively (Fig. 2B). Both the mutations are distant and not involved in any interaction.

Recently, two existing drugs talampicillin and lurasidone have shown binding energies of -11.17 Kcal/mol each and 2 drug-like compounds ZINC000015988935 and ZINC000103558522 exhibited binding energies of -12.39 and -12.36 Kcal/mol which suggests be 3CL Mpro protease inhibitors.[6] We observed that in the presence of H2Ocat the His41 and Asp187 refrained to involve the direct H-interaction. In a study, candidates with binding energies -6.1 to -7.75 kcal/mol were suggested better inhibition than nelfinavir based on the target interactions[7] and among the 36 tested deriva-

Abbreviations: 3CL, 3C-like protease; Mpro, main protease; vdW, van der Waals; CC50, half-maximum cytotoxic concentration; H-bond, hydrogen bond.

https://doi.org/10.1016/j.jinf.2022.02.012

Table 1
List of the scores and interactions retrieved during docking analyses.

Name/Zinc ID	S-score	Hydrogen bonds	Van der Waals and Hydrophobic interactions
Silymarin	-15.0411	Thr26, Asn142, Ser144, Cys145, His163	Thr24, Thr25, Phe140, Leu141, Gly143, Glu166
Ferulic Acid	-10.6320	Leu141, Gly143, Ser144, Cys145, His163, Glu166	Phe140, Asn142, Met165
p-coumaric acid	-10.7634	Phe140, Cys145, GLU166, HIS172	Leu141, Asn142, Gly143, Ser144, His163
ZINC64219754	-11.6969	His41, Gly143	Leu27, Met49, Phe140, Leu141, Asn142, Cys145, His164, Met165, Glu166, Arg188, Gln189, Thr190, Gln192
ZINC64219742	-11.1067	His41, Cys145	Thr25, Thr26, Leu27, Cys44, Thr45, Ser46, Met49, Phe140, Leu141, Asn142, Gly143, Ser144, His163, His164, Glu166
ZINC64219736	-10.7840	His41, Asn142, Gly143, His164	Leu27, Phe140, Leu141, Gly143, Ser144, Cys145, His163, Met165, Glu166

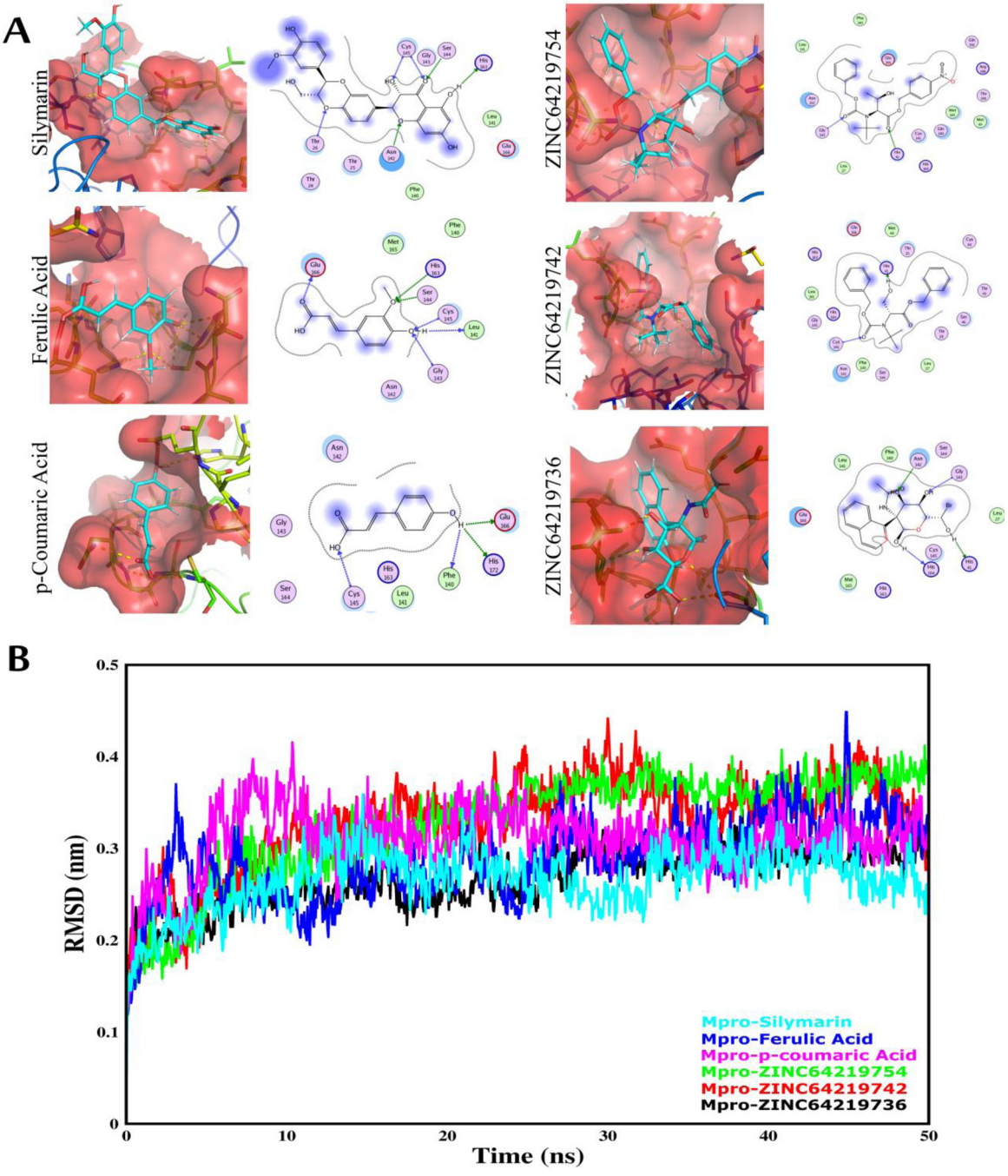

Fig. 1. Docking and Simulation Status of the 3CL Mpro Complexes. A. Ball and stick representation of silymarin, p-coumaric acid, ferulic acid, ZINC64219736, ZINC64219742 and ZINC64219754 interactions in the active-pocket of 3CL Mpro, shown in surface representation. Right panel describes the exact details of the interaction in 2D representation of the interaction is mentioned. Green and blue arrows represent the H-bond contact with backbone and side chain atoms of amino acids. B. Root-mean square deviation of the tested complexes across the 50 ns of simulation. Each complex is mentioned by its respective color.

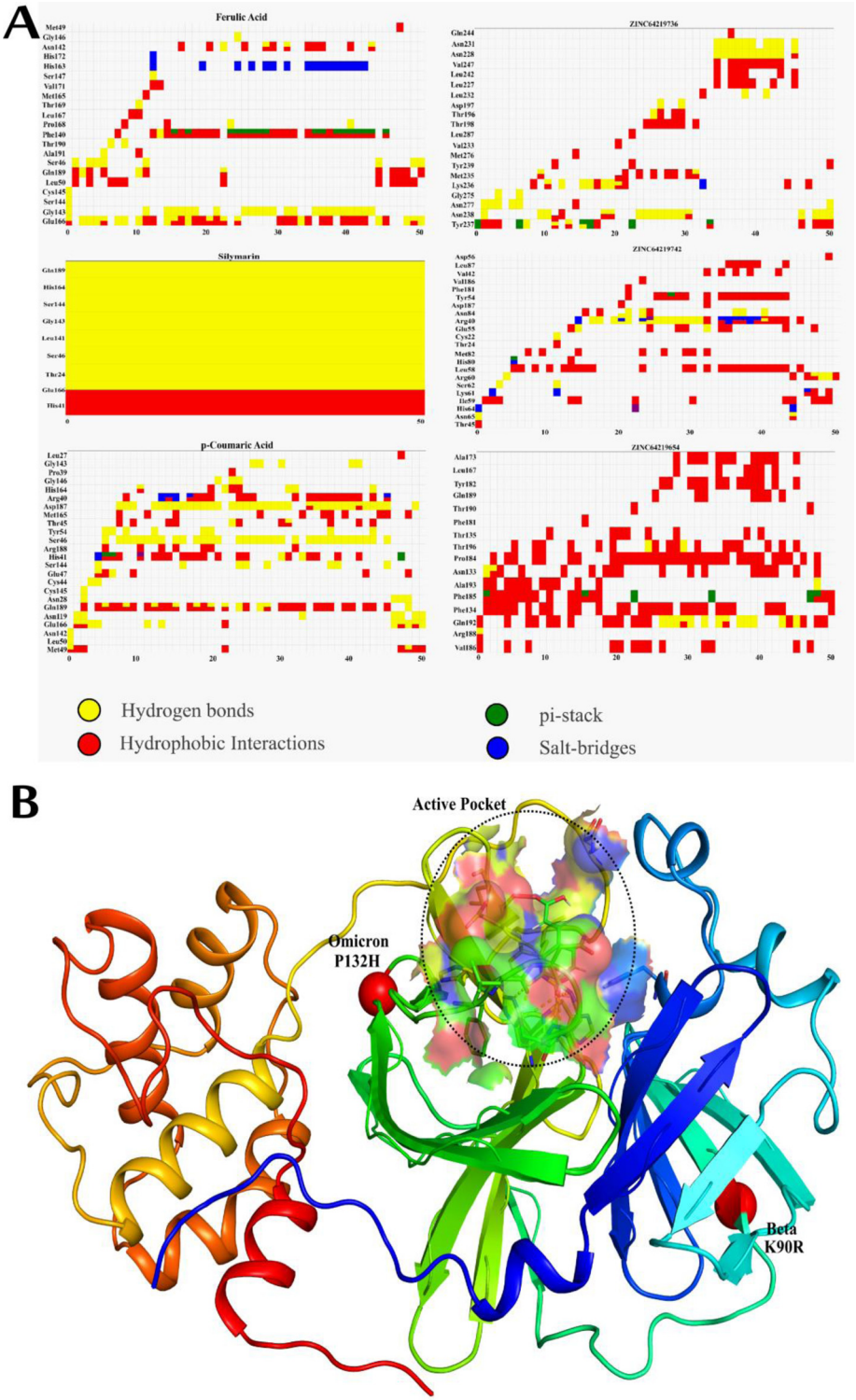

Fig. 2. Nature of interaction during simulation of 50 ns. A. Four types of interactions were observed, hydrogen bonds (yellow), hydrophobic interaction (red), pi-stacking (green) and salt-bridges (blue). Interacting amino acids are mentioned on the Y-axis where X-axis represents time period in simulation. B. Representation of mutation in SARS-CoV-2 variants. Red color spheres indicate the location of the observed mutation in Omicron and Beta Variant, in relation to the active pocket vicinity, shown in surface representation.

tives 20c, 24c, 30c, 34c, 35c, and 36c were identified best inhibitors based on the target receptor interactions with Gln189, Cys145, and His41 found significant. Derivatives of 2.5-diaminobenzophenone chosen molecules that achieved hydrophobic and vdW interactions with Thr25, Thr26, Leu27, Cys44, Thr45, Ser46, Met49, Phe140, Leu141, Asn142, Gly143, Ser144, His163, residues and H-bond interactions with residues His41, Leu141, Gly143, Ser144, Cys145, His163 and His164 were suggested potential candidates.[8]

Silymarin could also inhibit the dengue virus *in vitro* and were well tolerated in Vero cells with a half-maximum cytotoxic concentration (CC50) of 749.70 µg/mL against DENV-3, and prevented

viral entry (72.46%) into the cells with binding to the viral envelope.[9]

Overall, we further suggest six possible candidates and particularly silymarin that attained 15.0411Kcal/mol in docking and gained further fitness in terms of H-bonds in the pocket as compared to the other five candidates, suggesting the potent clinically targeting omicron through main protease 3CL Mpro besides targeting entry.[10]

Ethics approval and consent to participate

N/A.

Consent for publication

N/A.

Data sharing statement

All the data materials mentioned are available.

Funding

No funding is claimed.

Declaration of Competing Interest

Authors declare no conflict of interest.

Acknowledgements

We thank Nazarbayev University Faculty-Development Grants Program (ID: 40018290; 11022021FD2920 and 16797152).

References

1. Deng L, et al. Arbidol combined with LPV/r versus LPV/r alone against corona virus disease 2019: a retrospective cohort study. *J Infect* 2020;**81**(1):e1–5.
2. Li W, et al. SARS-CoV-2 Nsp5 activates NF-kappaB pathway by upregulating SUMOylation of MAVS. *Front Immunol* 2021;**12**:750969.
3. Liu CH, et al. Antiviral activities of silymarin and derivatives. *Molecules* 2019;**24**(8):1–15.
4. Musarra-Pizzo M, et al. Antiviral activity exerted by natural products against human viruses. *Viruses* 2021;**13**(5):1–30.
5. Costanzi E, et al. Structural and biochemical analysis of the dual inhibition of MG-132 against SARS-CoV-2 main protease (Mpro/3CLpro) and human cathepsin-L. *Int J Mol Sci* 2021;**22**(21).
6. Elmezayen AD, et al. Drug repurposing for coronavirus (COVID-19): in silico screening of known drugs against coronavirus 3CL hydrolase and protease enzymes. *J Biomol Struct Dyn* 2021;**39**(8):2980–92.
7. Sargolzaei M. Effect of nelfinavir stereoisomers on coronavirus main protease: molecular docking, molecular dynamics simulation and MM/GBSA study. *J Mol Gr Model* 2021;**103**:107803.
8. Ouassaf M, et al. Combined docking methods and molecular dynamics to identify effective antiviral 2, 5-diaminobenzophenonederivatives against SARS–CoV-2. *J King Saud Univ Sci* 2021;**33**(2):101352.
9. Low ZX, et al. Antiviral activity of silymarin and baicalein against dengue virus. *Sci Rep* 2021;**11**(1):21221.
10. Kazybay B, Ahmad A, Mu C, Mengdesh D, Xie Y. Omicron N501Y mutation among SARS-CoV-2 lineages: insilico analysis of potent binding to tyrosine kinase and hypothetical repurposed medicine. *Travel Med Infect Dis* 2022;**45**:102242 Jan-FebEpub 2021 Dec 17. PMID: 34929375; PMCID: PMC8677628. doi:10.1016/j.tmaid.2021.102242.

Aamir Saeed, Basharat Ahmad, Sidra Majaz, Faisal Nouroz, Ashfaq Ahmad*
Department of Bioinformatics, Hazara University, Mansehra 21300, Pakistan

Yingqiu Xie*
Biology Department, Nazarbayev University, Nur-Sultan 010000, Kazakhstan

*Corresponding authors.
E-mail addresses: ashfaq.binfo@hu.edu.pk (A. Ahmad), yingqiu.xie@nu.edu.kz (Y. Xie)